
Spectra of pathogens predict lethality of blue light photo-inactivation

David M. Harris

Rutgers School of Dental Medicine, Newark, NJ; Bio-Medical Consultants & Associates, Inc., Canandaigua, NY
California State University Chico, Chico, CA, USA

ABSTRACT

Whole-cell spectra of human pathogens are examined to identify species-specific wavelengths of maximum light absorption. It is presented how these data relate to clinical efficacy for antimicrobial phototherapies. Twelve species of microorganisms were cultured to exponential growth then processed and suspended in a scattering solution. Diffuse reflectance from the sample was delivered to two spectrometers that covered a spectral range of 370nm to 1200nm. Reflectance spectra were converted to relative absorbance. Absorbance spectra from multiple trials were averaged to produce a representative spectrum for each species. All pathogens studied demonstrated an absorbance spectrum with a primary component in the range 405-426 nm and 1-4 secondary components in the range 445-636 nm. Antibiotic-resistant and antibiotic-sensitive strains of *Pseudomonas aeruginosa* (*Pa*) had identical absorbance spectra. Whole-cell spectra support the hypothesis that a pathogen's absorbance is directly related to efficacy of photoinactivation. The spectral signatures in all pigmented bacteria tested appear to be that of various combinations of *in situ* porphyrins. The knowledge of the absorption spectrum of a given pathogen provides a logical start for selecting the appropriate light source for a clinical trial.

Key words: antimicrobial phototherapy; antibiotic resistance; whole-cell spectroscopy.

***Running Head:**

Spectra of pathogens

Corresponding author:

David M. Harris, Bio-Medical Consultants, Inc., Canandaigua, NY.

Telephone: 510.502.3345.

E-mail: bmcinc@comcast.net

Laser Therapy

©Copyright: the Author(s), 2023

Licensee PAGEPress, Italy

Laser Therapy 2023; 30:314

doi:10.4081/lj.2023.314

Introduction

In 2005 Dr. Abigail Salyers predicted that the “Revenge of the Microbes: How Bacterial Resistance is Undermining the Antibiotic Miracle”¹ would soon be upon us. Eighteen years after this prediction, Salyers’ warning has become reality and is gaining momentum at a disturbing rate.^{2,3} The increasing prevalence of bacteria that are resistant to antibiotics has become a serious global health care issue and the need for alternative therapies that may not evoke drug resistance has become an imperative. Antimicrobial phototherapies may provide an alternative. This study applies whole-cell diffuse reflection spectroscopy to provide a physical basis for development of a dosimetry for a clinical antimicrobial phototherapy.^{4,5} A clinical action spectrum for a certain phototherapy is produced by testing various wavelengths of light and quantifying some clinical outcome. Peaks in the action spectrum indicate wavelengths that are the most clinically effective. We test the idea that the germicidal action spectrum, or the effectiveness of each wavelength in killing some pathogen, is based on the absorption efficiency of the whole-cell at that wavelength. To this end, the absorption spectra of *in vitro* microorganisms were collected with diffuse reflection spectroscopy⁶ to identify peak absorption wavelengths of planktonic suspensions of human pathogens. These spectral components have revealed the areas of peak absorbance with potential to destroy a specific pathogen, the “Achilles wavelength” for that species. Whole-cell spectra are provided for twelve different species.

Materials and Methods

Safety

Good laboratory practices and standard microbiology methods were followed in this study. The growth and preparation of samples was done within a BSL 2 microbiology laboratory. Samples were prepared and subjected to testing within a biohazard safety cabinet. Used samples and materials were autoclaved and disposed of according to protocol.

Selection of bacterial species

A variety of known human pathogens were selected for spectroscopic evaluation. Care was taken to ensure a va-

riety of cellular morphologies were included in order to observe possible differences in resulting spectra that might be attributed to gram reaction, cell shape and size, and pigment production. *L. brevis* is not a known pathogenic species, but was included as a negative control for the presence of cytochromes. Some of the samples were used in previous studies and obtained from the California State University Chico, Department of Biology archives. Standardized American Type Culture Collection (ATCC) and National Collection of Type Cultures (NCTC) strains were obtained from Microbiologics, Inc. (St. Cloud MN 56303).

Antibiotic resistance

Differences in spectral components were evaluated for different strains of *P. aeruginosa*, that were either sensitive or resistant to traditional antibiotics. *P. aeruginosa* ATCC 25619 is a Carbenicillin and vancomycin resistant clinical isolate from a cystic fibrosis patient. NCTC 10662 is a non-mucoid human isolate with normal sensitivity to antibiotics. WT is a carbenicillin-resistant wildtype of unknown origin obtained from the CSU Chico archives.

Preparation of bacterial cultures for spectroscopy

Frozen glycerol stock cultures of the desired organism were plated onto trypticase soy agar (TSA) media for revival, purity assurance, and selection of a well-isolated colony. A single colony was transferred to 50mL sterile trypticase soy broth (TSB), and was incubated until exponential growth was achieved. Individual growth curves were performed on each species tested, and approximations of cellular concentration in 50mL TSB at *n* hours were obtained via absorption spectroscopy and serial dilution plating. Cultures to be used for spectroscopy were removed from incubation in mid-exponential growth phase and transferred into sterile centrifuge tubes for cellular harvest. Centrifugation at low gravities ensured that whole, undamaged cells were obtained. The resulting cell pellet was then washed 3 separate times with cold sterile phosphate buffered saline (PBS) to remove membrane debris and extracellular waste. After final wash, the supernatant was poured off and reconstituted with a known volume of sterile PBS to yield a “concentrated” culture to be used as a sample for spectroscopy.

Spectroscopy of microorganisms

Microbe absorbance spectra were determined by measuring diffuse reflectance from a scattering solution, adding the pathogen to the solution and measuring the change in reflectance. A decrease in reflectance is caused by the microbe absorbance. Detailed methods for recording absorption spectra of the bacteria, *Porphyromonas gingivalis* and *Prevotella intermedia*, using diffuse reflection spectroscopy were previously detailed (Harris, Jacques, Darveau, 2016, Appendix).⁶

A standard 3.3 mL 18-well plate in a darkened enclosure was used for spectroscopy. Wells were filled to capacity at 3.3 mL without a concave or convex surface. 2% homogenized, pasteurized cow milk was used as a scattering solution. The sample suspended in PBS was added to the scattering solution to produce 3.3 mL with a volume ratio of 3:1 scattering solution to sample suspended in PBS. Additional wells were also prepared; a "BASE" well was filled with 3.3mLs PBS to calibrate for stray light and specular reflectance and a "REFERENCE" well was filled with a 3:1 solution of 2% milk to PBS to evaluate background spectra with no pathogens present. In a single trial, wells were filled with a "BASE", a "REFERENCE" and a series of different "SAMPLES" consisting of different species, species strains, cell concentrations, cultures raised in different media, etc. up to 16 wells.

The light source was a halogen lamp (150W Sylvania 54753 - EJA) delivered through a 0.5cm diameter optical fiber bundle that was positioned to deliver light perpendicular to the sample surface. The short wavelength cut-off of the Halogen lamp was 410nm, so blue light from an LED (center WL: 390nm; half max 375-405nm) was introduced into the delivery fiber to examine spectral components in the blue light range. The LED/halogen intensity ratio was determined that minimized effects of fluorescence excitation. Each well was placed in the exact same position under the light source. The collection fiber viewed diffuse reflections from the well at a 45° angle to reduce specular reflections. The bifurcated fiber delivered the signal to two spectrometers (B&W Tek BRC11P-VIS and BTC261E-NIR, B&W Tek, Newark, DE 19713).

Spectra were collected using the B&WSpec 3.27 software at a sample rate of 135kHz over an integration time of 750ms. The software operating in multi-channel mode combined the signals from the two spectrometers

into a single file that covered a spectral range of 380nm-1400nm with a resolution of 0.67nm.

Analysis

The well with just PBS is called "BASE," the well with scattering solution plus PBS with no added absorber is called "REF" and the wells with scattering solution plus pathogen suspended in PBS is the "SAMPLE." The percent diffuse reflectance (R) is calculated:

$$R = \frac{\text{SAMPLE} - \text{BASE}}{\text{REF} - \text{BASE}}$$

Microbe spectra are plots of relative absorbance. Following the Lambert-Beer law reflectance (R) is converted to relative absorbance (A) as:

$$A = \log_{10} (1/R)$$

Component amplitude and peak wavelengths showed trial-to-trial variance in subsequent passes from the same stock culture. Results from at least three trials were averaged to obtain the representative spectra shown in the Results. Figure 1 shows four individual trials for *M. luteus*, *C. albicans*, *S. aureus* and *E. coli* and their representative spectrum. Differences in spectral component wavelengths across pathogen species were evaluated and within species between antibiotic-resistant and antibiotic-sensitive strains.

Results

Species tested

Figure 2 represents a library of twelve microbe spectra. All pathogens studied demonstrated an absorbance spectrum with a primary component in the range 405-426nm and 1-4 secondary components in the range 445-636nm (Table 1).

Spectral components

The primary component was more variable than secondary components. Table 2 lists for the three bacteria, *P. aeruginosa*, *K. pneumoniae* and *E. coli*, the average primary and secondary peak wavelengths, the wavelength

standard deviation and the sample size for each calculation. The analysis of *P. aeruginosa* peak wavelengths from 26 separate cultures showed that secondary components at 552nm and 524nm had a standard deviation (SD) of 1-2nm, whereas the primary peak SD was 4.3nm. Similar results were seen for *K. pneumoniae* (primary peak SD=10.86nm, n=11) and *E. coli* (primary peak SD=4.19, n=8). There were considerable species-to-species differences in spectral component relative absor-

bance amplitudes for samples with similar cell counts. In Figure 3A spectral amplitudes are compared for suspensions of *P. aeruginosa* and *E. coli* with similar cell concentrations (5×10^9 CFU/mL).

Resistance of *Pseudomonas aeruginosa*

Spectra were obtained from 3 different strains of *P. aeruginosa*. ATCC 25619 demonstrated resistance to car-

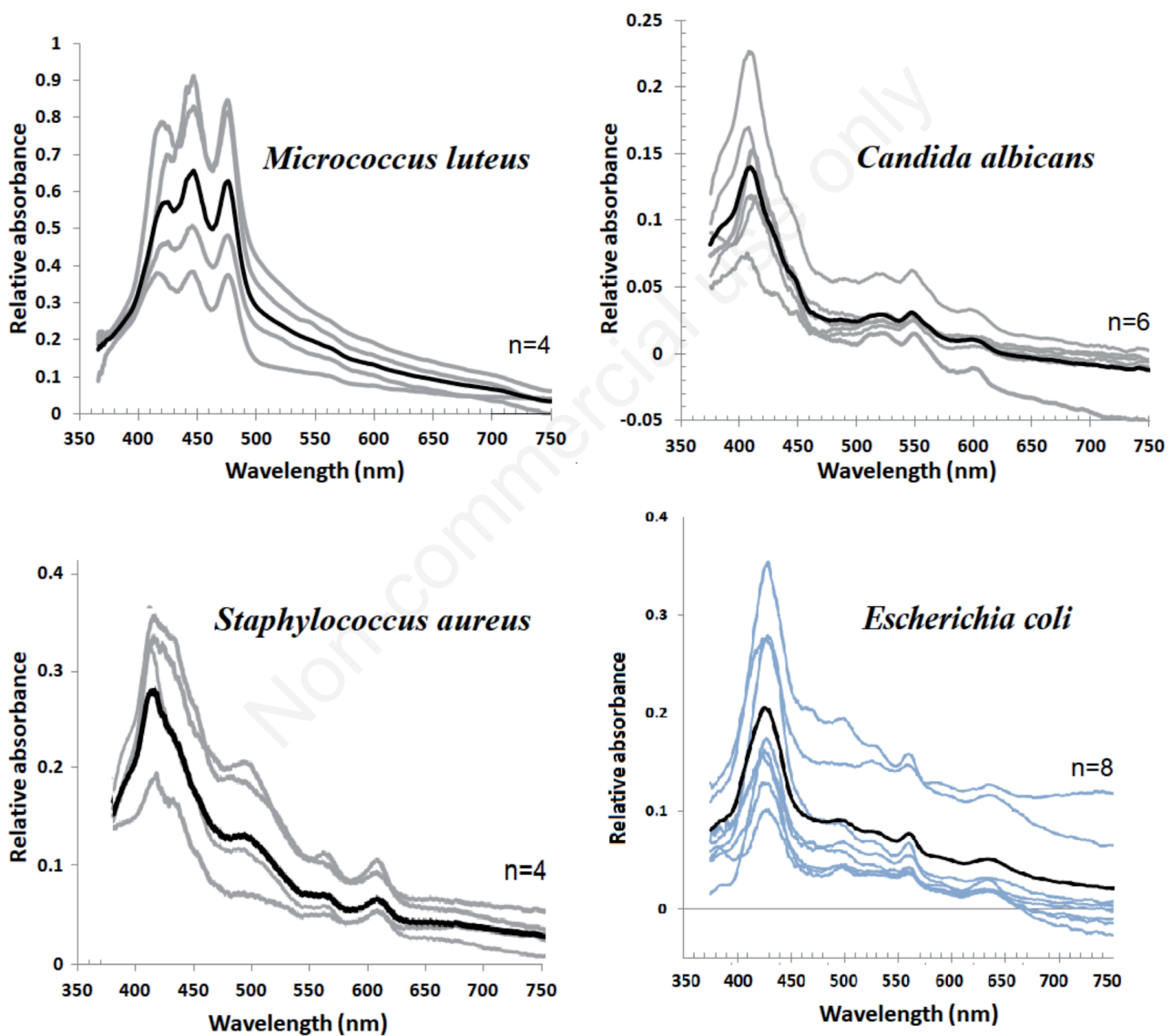


Figure 1. Diffuse reflection spectra of the microbes: *M. luteus*, *C. albicans*, *S. aureus* and *E. coli*. Separate trials (gray) are averaged to produce a representative absorbance spectrum (black).

benicillin and vancomycin. NCTC 10662 had normal sensitivity to both carbenicillin and vancomycin. WT, a wild type of unknown origin, was sensitive to carbenicillin and resistant to vancomycin. Figure 3B compares spectra from all three strains from a single trial. In nine replicates of this experiment, there were no consistent differences in component peak wavelengths among strains.

Discussion

Component amplitudes are affected by many factors

Apart from the influence of scattering and fluorescence, we assume that a whole-cell spectral component's ampli-

tude is a convolution of many factors including the relative absorption spectra of a variety of endogenous chromophores, the intracellular chromophore concentration(s), the typical cell volume and the cell concentration in the sample.

Since many bacteria scavenge heme to synthesize their own porphyrins, the cultivation procedure affects intracellular porphyrin content. Factors include cultivation time, passage number and the availability of certain nutrients.⁷ For example, *Porphyromonas gingivalis* was cultured with a low to high gradient of hemin concentrations in the growth media.⁶ The cultures showed the same gradient of both light to dark pigmentation and a systematic increase in general absorption in the wavelength band of hemin absorption.

Cell size, shape, surface features and spatial arrangement

Table 1. Peak wavelengths (nm) of spectral components. IR: infrared.

Species	1 ^o	400-499	500-599	600-699	IR
<i>Bacillales Bacillus cereus (Bc)</i> ATCC 14579	414	*	523 546	607	*
<i>Actinomycetales Cutibacterium acnes (C acn)</i> ATCC 6919	405	*	522 542	*	*
<i>Corynebacteriaceae Corynebacterium xerosis (Cx)</i> ATCC 373	418	465 491	593	*	*
<i>Enterobacteriales Escherichia coli (Ec)</i> ATCC 11775	426	497	527 560	636	*
<i>Enterobacteriales Klebsiella pneumoniae (Kp)</i> ATCC 31488	426		528 559	632	*
<i>Lactobacillales Lactobacillus brevis (Lb)</i> ATCC 14869	*	*	*	*	*
<i>Micrococcales Micrococcus luteus (Ml)</i> ATCC 4698	423	445 475	*	*	*
<i>Mycobacteriaceae Mycobacterium smegmatis (Ms)</i> ATCC 19420	407	497	*	*	*
<i>Neisseriales Neisseria mucosa (Nm)</i> ATCC 19695	413	*	522 549	*	*
<i>Pseudomonadaceae Pseudomonas aeruginosa (Pa)</i> ATCC 25619	415	*	523 552	*	*
<i>Bacillales Staphylococcus aureus (Sa)</i> ATCC BAA-2312	410	486	553	600	*
<i>Saccharomycetales Candida albicans (C alb)</i> ATCC 10231	410	*	522 547	600	1030

Table 2. Peak wavelength (nm) variance. The variance in the peak wavelength of the primary component was greater than secondary components. The sample size varies for each component because trials with low cell counts did not always show secondary components. SDEV: standard deviation; N: sample size.

Species	WL 1	WL 2	WL 3	WL 4	WL 5
<i>Ec</i>	425.5	496.9	527.0	559.5	632.8
SDEV	4.19	2.51	1.09	0.96	2.51
N	8	8	6	8	8
<i>Kp</i>	426.3	528.0	559.0	631.5	
SDEV	10.86	2.34	0.67	1.98	
N	11	6	9	8	
<i>Pa</i>	414.8	523.4	552.1		
SDEV	4.26	1.16	0.99		
N	26	21	21		

will affect differences in general spectral amplitude due to light scattering. Attenuation due to scattering is recorded as an increase in absorbance. *L. brevis* is appar-

ently devoid of cytochromes as its fermentative metabolism does not utilize cytochromes in a membrane electron transport system. This is evidenced by the absence

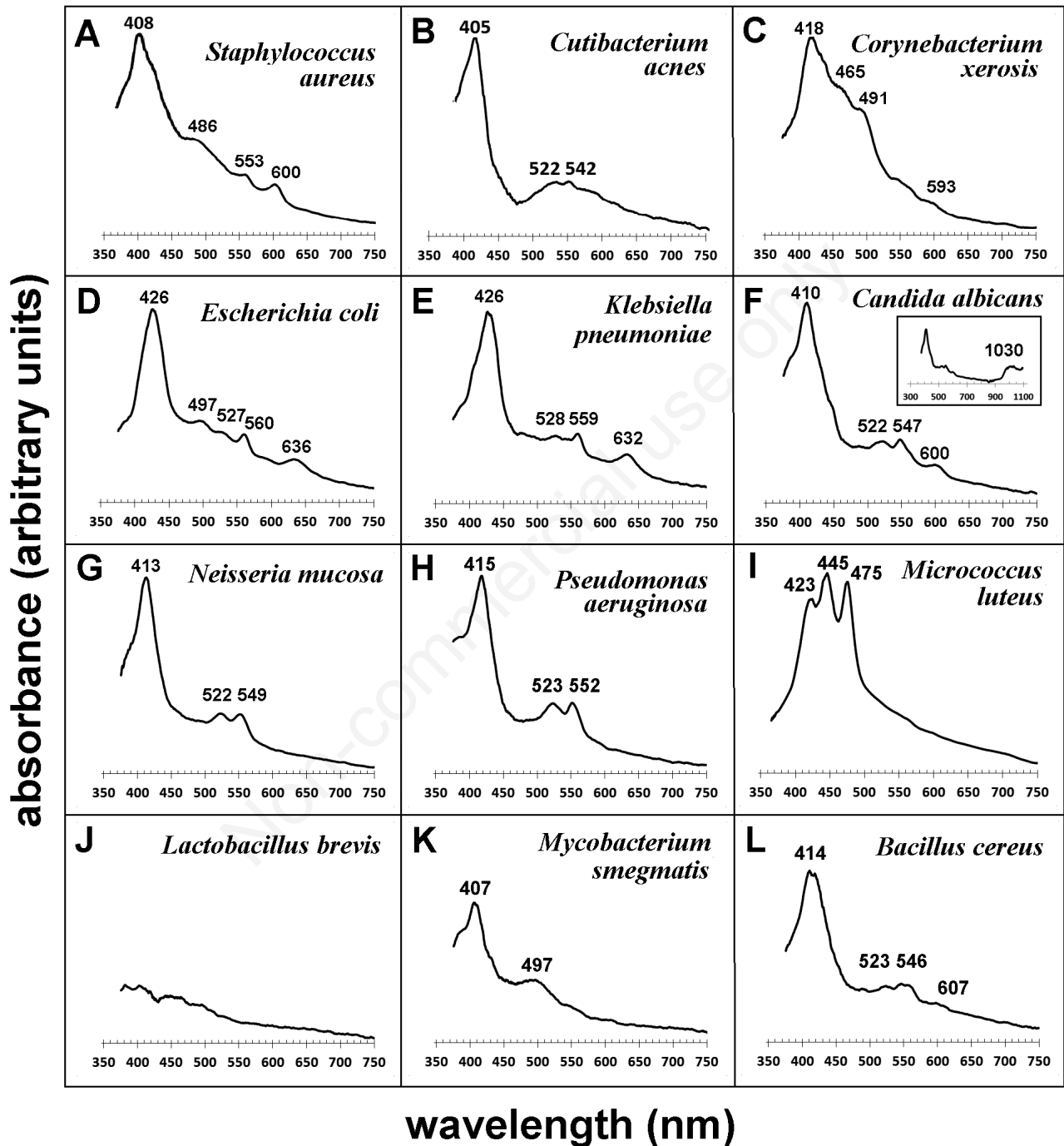


Figure 2. Absorbance spectra of microbes.

of a porphyrin signature in the *L. brevis* spectrum (Figure 2J). Consequently, the *L. brevis* spectrum probably demonstrates the general effect of light scattering without absorption. A similar negative slope is observed in most of our spectra which are not corrected for effects of light scattering.

Component wavelengths reflect internal porphyrin concentrations

The pathogens' absorbance spectra all had a primary component in the range 405-426nm and secondary components in the range 445-636nm (Table 2). Porphyrins possess an intense Soret band at approximately 400-420nm and several moderate Q-bands between 450 and 700nm. This similarity indicates that porphyrins are the primary chromophores responsible for the components observed in the whole-cell spectra.

P. aeruginosa demonstrated strong absorbance with definite peaks at 415, 523 and 552nm (Figures 2H-5; Table 1). *N. mucosa* has essentially the same components at 413, 522 and 549nm (Figure 2G; Table 1). The shape of these spectra match the absorption peaks of reduced cytochrome-c known to exist in high concentrations within the *P. aeruginosa* inner membrane.^{8,9} This suggests the hypothesis that the dominant chromophore of *P. aeruginosa* is, specifically, membrane-bound cytochrome-c. The in-

tracellular location of the photosensitizer is important. Damage directly to the energy producing inner membrane will be fatal to the cell. The photodynamic reaction that produces singlet oxygen has a 4 μs lifetime within a localized 0.2 μm diameter volume.¹⁰ Consequently, membrane-bound chromophores, such as cytochrome-c should improve the efficacy of antimicrobial blue light (aBL) applied to *P. aeruginosa* infections.¹¹

Spectra of pathogens predict germicidal efficacy

The results of *in vitro* susceptibility studies indicate that *C. albicans* can be selectively inactivated by intense light in the wavelength range of 405-420nm.¹²⁻¹⁶ Wang *et al.*¹⁶ measured *C. albicans* culture survival rates following irradiation by three different wavelengths: 405, 415 and 440nm. All cultures were treated with the same fluence of 50 mW/cm² for 900 seconds for a total light dose of 45 J/cm². In Figure 4A the relative pathogen absorbance is compared with survival rate (red dots) at each of these wavelengths. In this case; the *C. albicans*' absorbance spectrum matches the lethality action spectrum. Figure 4A illustrates an inverse relationship between absorbance and survival: the greater the absorbance the lower the survival rate.

Staphylococcus aureus is also sensitive to inactivation by blue light.^{17,18} Maclean *et al.*¹⁹ exposed culture plates of

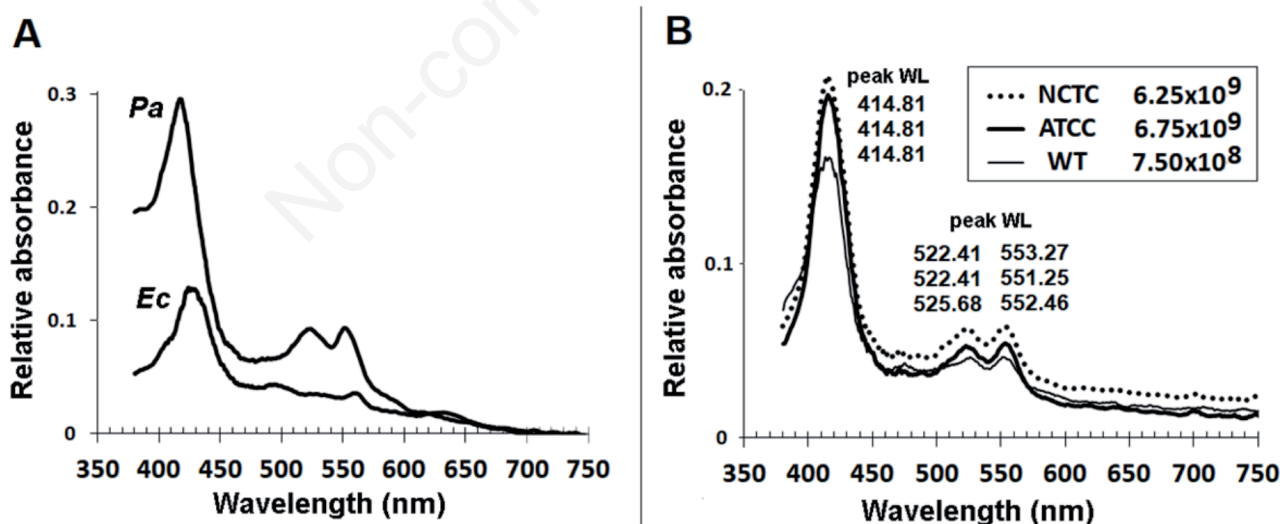


Figure 3. A. Spectra of *Pseudomonas aeruginosa* (*Pa*) and *Escherichia coli* (*Ec*) with similar cell concentrations (5X10⁹) showing a difference in relative absorbance. B. Spectra of three different strains of *P. aeruginosa* with varying sensitivity to chemical antibiotics. No differences in component wavelengths were observed.

S. aureus to 10nm bandwidths of light with center wavelengths from 400 to 430nm, with a light dose of 23.5 J/cm². They measured log₁₀ reduction in CFU. Figure 4B shows their data compared with the primary component of the *S. aureus* spectrum. Maximum germicidal efficacy coincides with the absorbance peak of the primary component in the *S. aureus* whole-cell spectrum.

Dissecting whole-cell spectra

There are several different modes of selective photoantiseptis for the treatment of bacterial and fungal infections. One mode is selective thermal ablation. High power density infrared light (800-1064nm) is used to selectively thermally ablate pigmented oral pathogens²⁰⁻²³ or toenail fungi.^{24,25} A different photophysical process, antimicrobial photodynamic therapy (aPDT), requires delivery of an exogenous photosensitizer drug that is selectively taken up by the pathogen. Destruction is a non-thermal photoinactivation through a low energy photochemical

reaction.²⁶ Antimicrobial blue light (aBL) is like aPDT but relies on endogenous chromophores as photosensitizers. aBL is considered as a separate clinical approach from aPDT since it does not require a drug.

Each of these therapies depends on the identity of a particular wavelength of light that matches the absorption of the target but is not absorbed by normal surrounding tissues. In this study we screened pigmented pathogens to identify potential treatment modalities for development of clinical applications. In order to translate from bench to clinic, it is shown that the pathogen's absorbance spectrum predicts the germicidal action spectrum. If the clinical outcome is "bacterial reduction" then pathogen absorbance as a function of wavelength also represents the clinical action spectrum.²⁷ Light in the Soret region of the absorption spectra of porphyrins is efficient for killing bacteria.^{11,12,28} The current thinking is that aBL targets endogenous porphyrins and results in photoinactivation of membrane function.^{11,29-33} As seen in the spectra (Figure 2), the por-

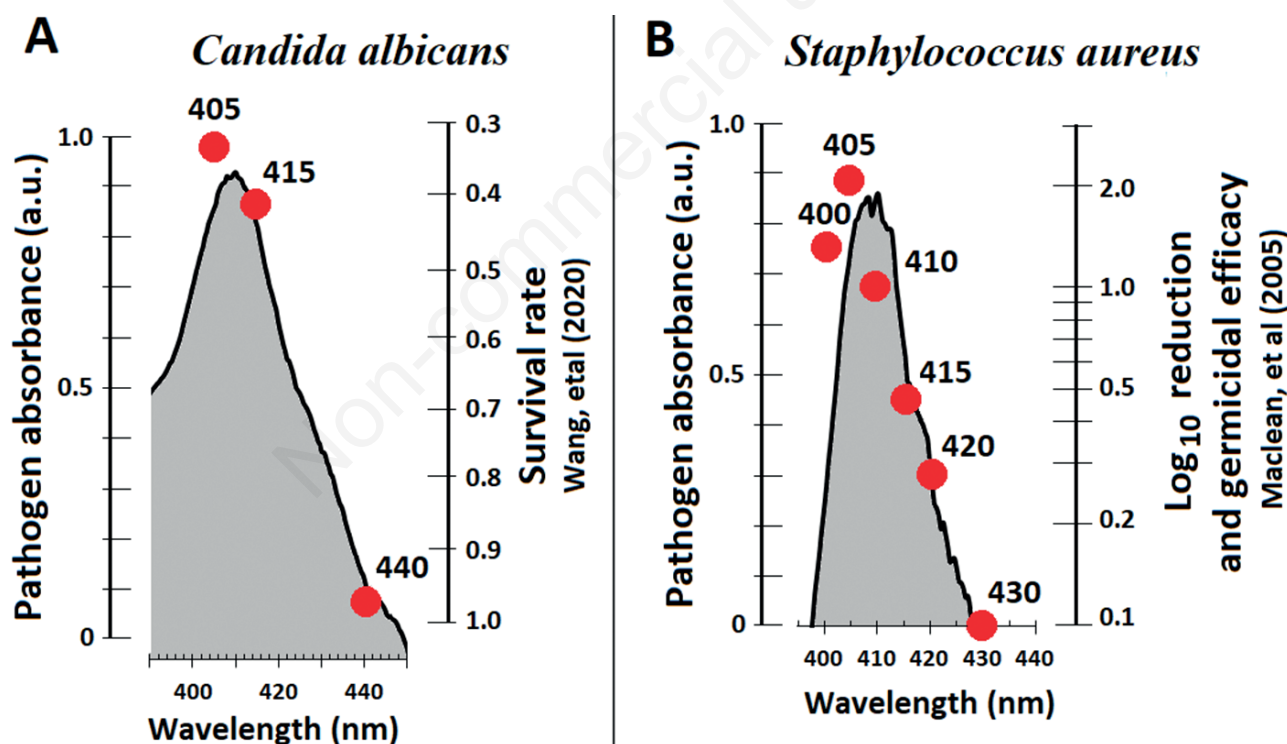


Figure 4. Pathogen absorbance is directly related to inverse survival rate, bacterial reduction and germicidal efficacy. A) The primary spectral component of *C. albicans* is compared to *C. albicans* survival rate following treatment with three different wavelengths. Greater relative absorbance relates to lower survival rates (red circles) (Survival data from Figure 1, Wang *et al.*, 2020); B) The primary spectral component of *S. aureus* is compared to the germicidal efficacy of a series of narrow band blue lights centered at the indicated wavelengths (other red circles) (Bacterial reduction data from Table 1, Maclean *et al.*, 2005).

phyrin signature dominates the whole-cell absorbance. The lethality of aBL appears to coincide with the absorption peak of the primary component (Figure 4), which presumably represents the Soret absorption bands of internal porphyrins. Hence, spectra from pathogens are consistent with the idea that the mechanism of action of aBL involves photodynamic inactivation through endogenous porphyrins. There may be either one dominant porphyrin as suggested for cytochrome-c in *P. aeruginosa* or a mixture of assorted porphyrins, as appears to be the case for *C. acnes* and *E. coli*.

Numerous combinations of cytochromes occur in most bacteria.^{34,35} *S. aureus*, *E. coli* and *K. pneumoniae* have the same primary peak wavelength (423-426nm) but a collection of different secondary components (Table 1). We suggest that these whole-cell spectra represent a convolution of the individual intracellular porphyrin spectral components. Thus, the whole-cell spectral component wavelengths reflect the cumulative acceptor molecules' energy states *in situ* that may not be the same as measurements of extracted porphyrins.

Many aBL reports assume 405nm to be the most effective germicidal wavelength.^{32,33,36} Whole-cell peak wavelengths were usually in the range of 405-415nm, but some spectra suggest that longer wavelengths near 420nm may be more effective for specific pathogens. If so, then the whole-cell absorbance spectrum may be a useful metric to develop the dosimetry for selectively targeting a specific strain or species.

Develop a clinical dosimetry

It is apparent from this survey that different species demonstrate a wide variety of spectral components and the Achilles wavelengths may vary from species to species. It follows that dosimetry for photoantiseptic needs to be species-specific. Porphyrin content evidently affects the photosensitivity of bacteria. Figure 3A shows greater relative absorbance of *P. aeruginosa* than *E. coli*. This corresponds to a difference in relative sensitivity.^{33,37} Certain pathogens like *P. aeruginosa*, *C. acnes* and *C. albicans* have high concentrations of porphyrins, hence colonies formed by this class of organisms make suitable targets for aBL. Due to apparent lower whole-cell absorption, *E. coli*, *M. smegmatus* and *B. cereus* would require longer treatment times and might be less suitable for this treatment modality unless sensitized exogenously.

For example, the porphyrin content and the photosensitivity of *E. coli* can be enhanced in the presence of 5-aminolevulinic acid.^{7,35}

Conclusions

Whole-cell spectra support the hypothesis that the spectral signatures of all pathogens tested appear to be that of various combinations of *in situ* porphyrins. The tip of the whole-cell primary component coincides with the Soret absorption band of internal porphyrins and it also represents the location of maximum germicidal effect. Our data indicate that the optimal wavelength for aBL may be quite different for different species. This needs to be falsified or verified.

Whole-cell absorbance provides a bridge between photochemistry and phototherapy. Whole-cell spectroscopy may provide a screening modality to identify pathogens that are candidates for selective photoantiseptic. The knowledge of the absorption spectrum of a given pathogen then provides a logical start for selecting the appropriate light source for a clinical trial. Multi-species colonies are common and may require development of a multi-spectral protocol. An in-depth knowledge of the optical properties of biofilms³⁸ and of the surrounding tissues is also necessary to determine the final dosimetry for any specific application.⁵ Success of any treatment ultimately relies on the development of a medically sound protocol that can be integrated into an established practice.

Conflict of interest: the Author declares no conflict of interest.

Ethics approval and consent to participate: no ethical committee approval was required for this report, because this article does not contain any studies with human participants or animals.

Availability of data and material: digital format of spectra are available upon request.

Acknowledgements: Molly Tuttle and Dan Lomeli provided microbes for analysis. We thank Gordon Wolfe for providing bench space in his laboratory.

References

1. Salyers AA, Whitt DD. Revenge of the microbes: how bacterial resistance is undermining the antibiotic miracle. Washington, D.C: ASM Press; 2005. 186 p.
2. Donlan RM, Costerton JW. Biofilms: survival mechanisms of clinically relevant microorganisms. Clin Microbiol Rev 2002;15:167–93.
3. Olsen I. Biofilm-specific antibiotic tolerance and resistance. Eur J Clin Microbiol Infect Dis Off Publ Eur Soc Clin Microbiol 2015;34:877–86.
4. Reinisch L. Scatter-limited phototherapy: a model for laser treatment of skin. Lasers Surg Med 2002;30:381–8.
5. Reinisch L, Garrett CG, Courey M. A simplified laser treatment planning system: proof of concept. Lasers Surg Med 2013;45: 679–85.
6. Harris DM, Jacques SL, Darveau R. The Black Bug Myth: Selective photodestruction of pigmented pathogens. Lasers Surg Med 2016;48:706–14.
7. Fyrestam J, Bjurshammar N, Paulsson E, et al. Influence of culture conditions on porphyrin production in *Aggregatibacter actinomycetemcomitans* and *Porphyromonas gingivalis*. Photodiagnosis Photodyn Ther 2017;17:115–23.
8. Pettigrew GW, Moore GR. Cytochromes c: biological aspects. Berlin ; New York: Springer-Verlag; 1987. 282 p.
9. Goodhew CF, Wilson IB, Hunter DJ, Pettigrew GW. The cellular location and specificity of bacterial cytochrome c peroxidases. Biochem J 1990;271:707–12.
10. Lindig BA, Rodgers MAJ, Schaap AP. Determination of the lifetime of singlet oxygen in water-d2 using 9,10-anthracenedipropionic acid, a water-soluble probe. J Am Chem Soc 1980;102:5590–3.
11. Kato H, Komagoe K, Inoue T, et al. Structure–activity relationship of porphyrin-induced photoinactivation with membrane function in bacteria and erythrocytes. Photochem Photobiol Sci 2018;17:954–63.
12. Zhang Y, Zhu Y, Chen J, et al. Antimicrobial blue light inactivation of *Candida albicans*: *In vitro* and *in vivo* studies. Virulence 2016;7:536–45.
13. Leanse LG, Goh XS, Dai T. Quinine improves the fungicidal effects of antimicrobial blue light: implications for the treatment of cutaneous candidiasis. Lasers Surg Med 2020; 52:569–75.
14. Papageorgiou P, Katsambas A, Chu A. Phototherapy with blue (415 nm) and red (660 nm) light in the treatment of acne vulgaris: blue-red light treatment of acne. Br J Dermatol 2000;142:973–8.
15. Trzaska WJ, Wrigley HE, Thwaite JE, May RC. Species-specific antifungal activity of blue light. Sci Rep 2017;7:4605.
16. Wang T, Dong J, Yin H, Zhang G. Blue light therapy to treat candida vaginitis with comparisons of three wavelengths: an *in vitro* study. Lasers Med Sci 2020;35:1329–39.
17. Rosa LP, da Silva FC, Viana MS, Meira GA. In vitro effectiveness of 455-nm blue LED to reduce the load of *Staphylococcus aureus* and *Candida albicans* biofilms in compact bone tissue. Lasers Med Sci 2016;31:27–32.
18. Bumah VV, Masson-Meyers DS, Cashin S, Enwemeka CS. Optimization of the antimicrobial effect of blue light on methicillin-resistant *Staphylococcus aureus* (MRSA) *in vitro*. Lasers Surg Med 2015;47:266–72.
19. Maclean M, MacGregor SJ, Anderson JG, Woolsey G. High-intensity narrow-spectrum light inactivation and wavelength sensitivity of *Staphylococcus aureus*. FEMS Microbiol Lett 2008;285:227–32.
20. Harris DM, Reinisch L. Selective photoantiseptis. Lasers Surg Med 2016;48:763–73.
21. Harris DM, White JM, Goodis H, et al. Selective ablation of surface enamel caries with a pulsed Nd:YAG dental laser. Lasers Surg Med 2002;30:342–50.
22. Bergmans L, Moisiadis P, Teughels W, Van Meerbeek B, Quirynen M, Lambrechts P. Bactericidal effect of Nd:YAG laser irradiation on some endodontic pathogens *ex vivo*. Int Endod J 2006;39:547–57.
23. Hatit YB, Blum R, Severin C, et al. The effects of a pulsed Nd:YAG laser on subgingival bacterial flora and on cementum: an *in vivo* study. J Clin Laser Med Surg 1996;14:137–43.
24. Harris DM, McDowell BA, Strisower J. Laser treatment for toenail fungus. In: Kollias N, Choi B, Zeng H, Malek RS, et al., eds. San Jose, CA; 2009. p. 71610M. Available from: <http://proceedings.spiedigitallibrary.org/proceeding.aspx?doi=10.1117/12.810193>
25. Gupta AK, Simpson FC, Heller DF. The future of lasers in onychomycosis. J Dermatol Treat 2016;27:167–72.
26. Wainwright M. Photodynamic antimicrobial chemotherapy (PACT). J Antimicrob Chemother 1998;42:13–28.
27. Karu TI, Kolyakov SF. Exact action spectra for cellular responses relevant to phototherapy. Photomed Laser Surg 2005;23:355–61.
28. Ashkenazi H, Malik Z, Harth Y, Nitzan Y. Eradication of *Propionibacterium acnes* by its endogenous porphyrins after illumination with high intensity blue light. FEMS Immunol Med Microbiol 2003;35:17–24.
29. Malik Z, Hanania J, Nitzan Y. New trends in photobiology bactericidal effects of photoactivated porphyrins — An alternative approach to antimicrobial drugs. J Photochem Photobiol B 1990;5:281–93.
30. Nitzan Y, Wexler HM, Finegold SM. Inactivation of anaerobic bacteria by various photosensitized porphyrins or by hemin. Curr Microbiol 1994;29:125–31.
31. Meffert H, Gaunitz K, Gutewort T, Amlong UJ. [Therapy of acne with visible light. Decreased irradiation time by using a blue-light high-energy lamp]. Dermatol Monatschrift 1990; 176:597–603.
32. Leanse LG, dos Anjos C, Mushtaq S, Dai T. Antimicrobial blue light: A 'Magic Bullet' for the 21st century and beyond? Adv Drug Deliv Rev 2022;180:114057.
33. Halstead FD, Hadis MA, Marley N, et al. Violet-blue light arrays at 405 nanometers exert enhanced antimicrobial activity for photodisinfection of monomicrobial nosocomial biofilms. Appl Environ Microbiol 2019;85:e01346-19.
34. Smith L. Bacterial cytochromes. Bacteriol Rev 1954;18:106–30.
35. Amin RM, Bhayana B, Hamblin MR, Dai T. Antimicrobial blue light inactivation of *Pseudomonas aeruginosa* by photoexcitation of endogenous porphyrins: *In vitro* and *in vivo* studies. Lasers Surg Med 2016;48:562–8.

-
36. Dai T, Gupta A, Huang YY, et al. Blue light rescues mice from potentially fatal *Pseudomonas aeruginosa* burn infection: efficacy, safety, and mechanism of action. *Antimicrob Agents Chemother* 2013;57:1238–45.
37. Ferrer-Espada R, Wang Y, Goh XS, Dai T. Antimicrobial blue light inactivation of microbial isolates in biofilms. *Lasers Surg Med* 2020;52:472–8.
38. Song HH, Lee JK, Um HS, et al. Phototoxic effect of blue light on the planktonic and biofilm state of anaerobic periodontal pathogens. *J Periodontal Implant Sci* 2013;43:72.

Non-commercial use only